Friction at Water / Ice-I_h interfaces: Do the Different Facets of Ice Have Different Hydrophilicity?

Patrick B. Louden and J. Daniel Gezelter *

*Department of Chemistry and Biochemistry, University of Notre Dame, Notre Dame, IN 46556

Submitted to Proceedings of the National Academy of Sciences of the United States of America

In this follow up paper of the basal and prismatic facets of the Ice-I_h/water interface, we present the pyramidal and secondary prismatic interfaces for both the quiescent and sheared systems. The structural and dynamic interfacial widths for all four crystal facets were found to be in good agreement, and were found to be independent of the shear rate over the shear rates investigated. Decomposition of the molecular orientational time correlation function showed different behavior for the short- and longer-time decay components approaching normal to the interface. Lastly we show through calculation of the interfacial friction coefficient that the basal and pyramidal facets are more hydrophilic than the prismatic and secondary prismatic facets.

ice | water | interface | contact angle | molecular dynamics

Abbreviations: QLL, quasi liquid layer; MD, molecular dynamics

The Ice-I_h/water quiescent interface has been extensively studied over the past 30 years by theory and experiment. Haymet *et al.* have done significant work characterizing and quantifying the width of these interfaces for the SPC,[111990Karim, Kay, and Haymet] SPC/E,[122002Gay, Smith, and Haymet, 132002Bryk and Haymet], CF1,[142001Hayward and Haymet, 152002Hayward and Haymet] and TIP4P[161988Karim and Haymet] models for water.[172004Bryk and Haymet, 182005Smith, Bryk, and Haymet, 192008Wilson and Haymet, 202010Wilson and Haymet] Nada and Furukawa have studied the the basal- and prismatic-water interface width[**?**] and crystal surface restructuring at temperatures approaching the melting point[**?**].

It is well known that the surface of ice exhibits a premelting layer at temperatures near the melting point, often called a quasi-liquid layer (QLL). Molecular dynamics simulations of the facets of ice-I_h exposed to vacuum performed by Conde, Vega and Patrykiejew have found QLL widths of approximately 10 Å at 3 K below the melting point[**?**]. Similarly, Limmer and Chandler have used course grain simulations and statistical field theory to estimated QLL widths at the same temperature to be about 3 nm[**?**]. Recently, Sazaki and Furukawa have developed an experimental technique with sufficient spatial and temporal resolution to visulaize and quantitatively analyze QLLs on ice crystals at temperatures near melting[**?**]. They have found the width of the QLLs perpindicular to the surface at -2.2^{o}C to be 3-4 Å wide. They have also seen the formation of two immiscible QLLs, which displayed different stabilities and dynamics on the crystal surface[**?**].

There is significant interest in the properties of ice/ice and ice/water interfaces in the geophysics community. Most commonly, the results of shearing two ice blocks past one another[**?**, **?**, **?**, **?**] or the shearing of ice through water[**?**, **?**]. Using molecular dynamics simulations, Samadashvili has recently shown that when two smooth ice slabs slide past one another, a stable liquid-like layer develops between them[**?**]. To fundamentally understand these processes, a molecular understanding of the ice/water interfaces is needed. Investigation of the ice/water interface is also crucial in understanding processes such as nucleation, crystal growth,[11992Han and Hale, 21995Granasy, 31995Vanfleet and Mochel] and crystal melting[41983Weber and Stillinger, 11992Han and Hale, 51996Sakai, 61996Sakai].

In a previous study[212013Louden and Gezelter], we investigated the basal and prismatic facets of an ice-I_h/water interface where the ice was sheared relative to the liquid. Using velocity shearing and scaling approach to reverse nonequilibrium molecular dynamics (VSS-RNEMD), simultaneous temperature and velocity gradients were applied to the system, allowing for measurment of friction and thermal transport properties while maintaining a stable interfacial temperature[**?**].

Paragraph here about hydrophobicity and hydrophilicity, maybe move up more in the paper as well. Talk about physically what it means for a surface to by hydrophobic or hydrophilic, and then we move into how do we define it (mathematically) and then measure the degree of wetting experimentally and theoretically.

The hydrophobicity or hydrophilicity of a surface can be described by the extent a droplet of water wets the surface. The contact angle formed between the solid and the liquid, θ, which relates the free energies of the three interfaces involved, is given by Young's equation.

$$\cos\theta = (\gamma_{sv} - \gamma_{sl})/\gamma_{lv} \qquad [1]$$

Here γ_{sv}, γ_{sl}, and γ_{lv} are the free energies of the solid/vapor, solid/liquid, and liquid/vapor interfaces respectively. Large contact angles ($\theta \gg 90^o$) correspond to low wettability and hydrophobic surfaces, while small contact angles ($\theta \ll 90^o$) correspond to high wettability and hydrophilic surfaces. Experimentally, measurements of the contact angle of sessile drops has been used to quantify the extent of wetting on surfaces with thermally selective wetting charactaristics[**?**, **?**, **?**], as well as nano-pillared surfaces with electrically tunable Cassie-Baxter and Wenzel states[**?**, **?**, **?**, **?**, **?**]. Luzar and coworkers

Significance

RJSM and ACAC developed the concept of the study. RJSM conducted the analysis, data interpretation and drafted the manuscript. AGB contributed to the development of the statistical methods, data interpretation and drafting of the manuscript.

Reserved for Publication Footnotes

have done significant work modeling these transitions on nanopatterned surfaces[**?**, **?**, **?**, **?**], and have found the change in contact angle to be due to the external field perturbing the hydrogen bonding of the liquid/vapor interface[**?**].

The resulting solid/liquid kinetic friction coefficients were reported, and displayed a factor of two difference between the basal and prismatic facets. In this paper we present the same analysis for the pyramidal and secondary prismatic facets, and show that the differential interfacial friction coefficients for the four facets of ice-I_h are determined by their relative hydrophilicity by means of dynamics water contact angle simulations.

Methodology

Water Model. Understanding ice/water interfaces inherently begins with the isolated systems. There has been extensive work parameterizing models for liquid water, such as the SPC[**?**], SPC/E[**?**], TIP4P[**?**], TIP4P/2005[**?**], (. . .), and more recently, models for simulating the solid phases of water, such as the TIP4P/Ice[**?**] model. The melting point of various crystal structures of ice have been calculated for many of these models (SPC[111990Karim, Kay, and Haymet, **?**], SPC/E[**?**, **?**, 122002Gay, Smith, and Haymet, 132002Bryk and Haymet, **?**, **?**, **?**, **?**, **?**], TIP4P[161988Karim and Haymet, **?**, **?**, **?**, **?**, **?**, **?**, **?**], TIP5P[**?**, **?**, **?**, **?**, **?**]), and the partial or complete phase diagram for the model has been determined (SPC/E[**?**, **?**, **?**], TIP4P[**?**, **?**, **?**], TIP5P[**?**, **?**]).

Haymet et al. have studied the quiescent Ice-I_h/water interface using the rigid SPC, SPC/E, TIP4P, and the flexible CF1 water models, and has seen good agreement for structural and dynamic measurements of the interfacial width. Given the expansive size of our systems of interest, and to compare with our previous work, we have chosen to use rigid SPC/E water model in this study.

Pyramidal and secondary prismatic system construction. The construction of the pyramidal and secondary prismatic systems follows that of the basal and prismatic systems presented elsewhere[212013Louden and Gezelter], however the ice crystals and water boxes were equilibrated and combined at 50K instead of 225K. The ice / water systems generated were then equilibrated to 225K. The resulting pyramidal system was $37.47 \times 29.50 \times 93.02$ Å with 1216 SPC/E[**?**] molecules in the ice slab, and 2203 in the liquid phase. The secondary prismatic system generated was $71.87 \times 31.66 \times 161.55$ Å with 3840 SPC/E molecules in the ice slab and 8176 molecules in the liquid phase.

Shearing simulations. The computational details performed here were equivalent to those reported in our previous publication[212013Louden and Gezelter]. The only changes made to the previously reported procedure were the following. VSS-RNEMD moves were attempted every 2 fs instead of every 50 fs. This was done to minimize the magnitude of each individual VSS-RNEMD perturbation to the system.

All pyramidal simulations were performed under the canonical (NVT) ensamble except those during which statistics were accumulated for the orientational correlation function, which were performed under the microcanonical (NVE) ensamble. All secondary prismatic simulations were performed under the NVE ensamble.

Droplet simulations. Here, we will calculate the contact angle of a water droplet as it spreads across each of the four ice I_h crystal facets in order to determine the surface's relative hydrophilicites. The ice surfaces were oriented so that the desired facet was exposed to the positive z dimension. The sizes and number of molecules in each of the surfaces is given in Table **??**. Molecular restraints were applied to the center of mass of the rigid bodies to prevent surface melting, however the molecules were allowed to reorient themselves freely. The water doplet to be placed on the surface contained 2048 SPC/E molecules, which has been found to produce agreement for the Young contact angle extrapolated to an infinite drop size[**?**]. The surfaces and droplet were equilibrated to 225 K, at which time the droplet was placed 3-5 Å above the surface at 5 unique locations. Each simulation was 5 ns in length and conducted in the NVE ensemble.

Results and discussion

Interfacial width. In the literature there is good agreement that between the solid ice and the bulk water, there exists a region of 'slush-like' water molecules. In this region, the water molecules are structurely distinguishable and behave differently than those of the solid ice or the bulk water. The characteristics of this region have been defined by both structural and dynamic properties; and its width has been measured by the change of these properties from their bulk liquid values to those of the solid ice. Examples of these properties include the density, the diffusion constant, and the translational order profile. [132002Bryk and Haymet, 111990Karim, Kay, and Haymet, 122002Gay, Smith, and Haymet, 142001Hayward and Haymet, 152002Hayward and Haymet, 161988Karim and Haymet]

Since the VSS-RNEMD moves used to impose the thermal and velocity gradients perturb the momenta of the water molecules in the systems, parameters that depend on translational motion may give faulty results. A stuructural parameter will be less effected by the VSS-RNEMD perturbations to the system. Due to this, we have used the local tetrahedral order parameter (Eq 5[212013Louden and Gezelter] to quantify the width of the interface, which was originally described by Kumar[222009Kumar, Buldyrev, and Stanley] and Errington[232001Errington and Debenedetti], and used by Bryk and Haymet in a previous study of ice/water interfaces.[**?**]

To determine the width of the interfaces, each of the systems were divided into 100 artificial bins along the z-dimension, and the local tetrahedral order parameter, $q(z)$, was time-averaged for each of the bins, resulting in a tetrahedrality profile of the system. These profiles are shown across the z-dimension of the systems in panel a of Figures 1 and 2 (black circles). The $q(z)$ function has a range of (0,1), where a larger value indicates a more tetrahedral environment. The $q(z)$ for the bulk liquid was found to be ≈ 0.77, while values of ≈ 0.92 were more common for the ice. The tetrahedrality profiles were fit using a hyperbolic tangent[212013Louden and Gezelter] designed to smoothly fit the bulk to ice transition, while accounting for the thermal influence on the profile by the kinetic energy exchanges of the VSS-RNEMD moves. In panels b and c, the resulting thermal and velocity gradients from an imposed kinetic energy and momentum fluxes can be seen. The verticle dotted lines traversing all three panels indicate the midpoints of the interface as determined by the hyperbolic tangent fit of the tetrahedrality profiles.

From fitting the tetrahedrality profiles for each of the 0.5 nanosecond simulations (panel c of Figures 1 and 2) by eq. 6[212013Louden and Gezelter],we find the interfacial width to be 3.2 ± 0.2 and 3.2 ± 0.2 Å for the control system with no applied momentum flux for both the pyramidal and secondary prismatic systems. Over the range of shear rates investigated,

0.6 ± 0.2 ms^{-1} $\rightarrow$ 5.6 ± 0.4 ms^{-1} for the pyramidal system and 0.9 ± 0.3 ms^{-1} $\rightarrow$ 5.4 ± 0.1 ms^{-1} for the secondary prismatic, we found no significant change in the interfacial width. This follows our previous findings of the basal and prismatic systems, in which the interfacial width was invarient of the shear rate of the ice. The interfacial width of the quiescent basal and prismatic systems was found to be 3.2 ± 0.4 Å and 3.6 ± 0.2 Å respectively, over the range of shear rates investigated, 0.6 ± 0.3 ms^{-1} $\rightarrow$ 5.3 ± 0.5 ms^{-1} for the basal system and 0.9 ± 0.2 ms^{-1} $\rightarrow$ 4.5 ± 0.1 ms^{-1} for the prismatic.

These results indicate that the surface structure of the exposed ice crystal has little to no effect on how far into the bulk the ice-like structural ordering is. Also, it appears that the interface is not structurally effected by shearing the ice through water.

Orientational dynamics. The orientational time correlation function,

$$C_2(t) = \langle P_2(\mathbf{u}(0) \cdot \mathbf{u}(t)) \rangle, \qquad [2]$$

helps indicate the local environment around the water molecules. The function begins with an initial value of unity, and decays to zero as the water molecule loses memory of its former orientation. Observing the rate at which this decay occurs can provide insight to the mechanism and timescales for the relaxation. In eq. [**2**], P_2 is the second-order Legendre polynomial, and $\mathbf{u}$ is the bisecting HOH vector. The angle brackets indicate an ensemble average over all the water molecules in a given spatial region.

To investigate the dynamics of the water molecules across the interface, the systems were divided in the z-dimension into bins, each ≈ 3 Å wide, and eq. [**2**] was computed for each of the bins. A water molecule was allocated to a particular bin if it was initially in the bin at time zero. To compute eq. [**2**], each 0.5 ns simulation was followed by an additional 200 ps NVE simulation during which the position and orientations of each molecule were recorded every 0.1 ps.

The data obtained for each bin was then fit to a triexponential decay with the three decay constants τ_{short} corresponding to the librational motion of the water molecules, τ_{middle} corresponding to jumps between the breaking and making of hydrogen bonds, and τ_{long} corresponding to the translational motion of the water molecules. An additive constant in the fit accounts for the water molecules trapped in the ice which do not experience any long-time orientational decay.

In Figures 3 and 4 we see the z-coordinate profiles for the three decay constants, τ_{short} (panel a), τ_{middle} (panel b), and τ_{long} (panel c) for the pyramidal and secondary prismatic systems respectively. The control experiments (no shear) are shown in black, and an experiment with an imposed momentum flux is shown in red. The vertical dotted line traversing all three panels denotes the midpoint of the interface as determined by the local tetrahedral order parameter fitting. In the liquid regions of both systems, we see that τ_{middle} and τ_{long} have approximately consistent values of $3-6$ ps and $30-40$ ps, resepctively, and increase in value as we approach the interface. Conversely, in panel a, we see that τ_{short} decreases from the liquid value of $72-76$ fs as we approach the interface. We believe this speed up is due to the constrained motion of librations closer to the interface. Both the approximate values for the decays and trends approaching the interface match those reported previously for the basal and prismatic interfaces.

As done previously, we have attempted to quantify the distance, $d_{pyramidal}$ and $d_{secondaryprismatic}$, from the interface that the deviations from the bulk liquid values begin. This was done by fitting the orientational decay constant z-profiles by

$$\tau(z) \approx \tau_{liquid} + (\tau_{wall} - \tau_{liquid}) e^{-(z - z_{wall})/d} \qquad [3]$$

where τ_{liquid} and τ_{wall} are the liquid and projected wall values of the decay constants, z_{wall} is the location of the interface, and d is the displacement from the interface at which these deviations occur. The values for $d_{pyramidal}$ and $d_{secondaryprismatic}$ were determined for each of the decay constants, and then averaged for better statistics (τ_{middle} was ommitted for secondary prismatic). For the pyramidal system, $d_{pyramidal}$ was found to be 2.7 Å for both the control and the sheared system. We found $d_{secondaryprismatic}$ to be slightly larger than $d_{pyramidal}$ for both the control and with an applied shear, with displacements of 4 Å for the control system and 3 Å for the experiment with the imposed momentum flux. These values are consistent with those found for the basal ($d_{basal} \approx 2.9$ Å) and prismatic ($d_{prismatic} \approx 3.5$ Å) systems.

Coefficient of friction of the interfaces. While investigating the kinetic coefficient of friction, there was found to be a dependence for μ_k on the temperature of the liquid water in the system. We believe this dependence arrises from the sharp discontinuity of the viscosity for the SPC/E model at temperatures approaching 200 K[**?**]. Due to this, we propose a weighting to the interfacial friction coefficient, κ by the shear viscosity of the fluid at 225 K. The interfacial friction coefficient relates the shear stress with the relative velocity of the fluid normal to the interface:

$$j_z(p_x) = \kappa[v_x(fluid) - v_x(solid)] \qquad [4]$$

where $j_z(p_x)$ is the applied momentum flux (shear stress) across z in the x-dimension, and v_x(fluid) and v_x(solid) are the velocities directly adjacent to the interface. The shear viscosity, $\eta(T)$, of the fluid can be determined under a linear response of the momentum gradient to the applied shear stress by

$$j_z(p_x) = \eta(T) \frac{\partial v_x}{\partial z}. \qquad [5]$$

Using eqs [**5**] and [**6**], we can find the following expression for κ,

$$\kappa = \eta(T) \frac{\partial v_x}{\partial z} \frac{1}{[v_x(fluid) - v_x(solid)]}. \qquad [6]$$

Here is where we will introduce the weighting term of $\eta(225)/\eta(T)$ giving us

$$\kappa = \frac{\eta(225)}{[v_x(fluid) - v_x(solid)]} \frac{\partial v_x}{\partial z}. \qquad [7]$$

To obtain the value of $\eta(225)$ for the SPC/E model, a $31.09 \times 29.38 \times 124.39$ Å box with 3744 SPC/E liquid water molecules was equilibrated to 225K, and 5 unique shearing experiments were performed. Each experiment was conducted in the NVE and were 5 ns in length. The VSS were attempted every timestep, which was set to 2 fs. For our SPC/E systems, we found $\eta(225)$ to be 0.0148 ± 0.0007 Pa s, roughly ten times larger than the value found for 280 K SPC/E bulk water by Kuang[**?**].

The interfacial friction coefficient, κ, can equivalently be expressed as the ratio of the viscosity of the fluid to the slip length, δ, which is an indication of how 'slippery' the interface is.

$$\kappa = \frac{\eta}{\delta} \qquad [8]$$

In each of the systems, the interfacial temperature was kept fixed to 225K, which ensured the viscosity of the fluid at the interace was approximately the same. Thus, any significant variation in κ between the systems indicates differences in the

'slipperiness' of the interfaces. As each of the ice systems are sheared relative to liquid water, the 'slipperiness' of the interface can be taken as an indication of how hydrophobic or hydrophilic the interface is. The calculated κ values found for the four crystal facets of Ice-I_h investigated are shown in Table I. The basal and pyramidal facets were found to have similar values of $\kappa \approx 0.0006$ (amu Å^{-2} fs^{-1}), while values of $\kappa \approx 0.0003$ (amu Å^{-2} fs^{-1}) were found for the prismatic and secondary prismatic systems. These results indicate that the basal and pyramidal facets are more hydrophilic than the prismatic and secondary prismatic facets.

Dynamic water contact angle.

Conclusion

We present the results of molecular dynamics simulations of the pyrmaidal and secondary prismatic facets of an SPC/E model of the Ice-I_h/water interface. The ice was sheared through the liquid water while being exposed to a thermal gradient to maintain a stable interface by using the minimally perturbing VSS RNEMD method. In agreement with our previous findings for the basal and prismatic facets, the interfacial width was found to be independent of shear rate as measured by the local tetrahedral order parameter. This width was found to be 3.2 ± 0.2 Å for both the pyramidal and the secondary prismatic systems. These values are in good agreement with our previously calculated interfacial widths for the basal (3.2 ± 0.4 Å) and prismatic (3.6 ± 0.2 Å) systems.

Orientational dynamics of the Ice-I_h/water interfaces were studied by calculation of the orientational time correlation function at varying displacements normal to the interface. The decays were fit to a tri-exponential decay, where the three decay constants correspond to the librational motion of the molecules driven by the restoring forces of existing hydrogen bonds (τ_{short} $\mathcal{O}$(10 fs)), jumps between two different hydrogen bonds (τ_{middle} $\mathcal{O}$(1 ps)), and translational motion of the molecules (τ_{long} $\mathcal{O}$(100 ps)). τ_{short} was found to decrease approaching the interface due to the constrained motion of the molecules as the local environment becomes more ice-like. Conversely, the two longer-time decay constants were found to increase at small displacements from the interface. As seen in our previous work on the basal and prismatic facets, there appears to be a dynamic interface width at which deviations from the bulk liquid values occur. We had previously found d_{basal} and $d_{prismatic}$ to be approximately 2.8 Å and 3.5 Å. We found good agreement of these values for the pyramidal and secondary prismatic systems with $d_{pyramidal}$ and $d_{secondaryprismatic}$ to be 2.7 Å and 3 Å. For all four of the facets, no apparent dependence of the dynamic width on the shear rate was found.

The interfacial friction coefficient, κ, was determined for each facet interface. We were able to reach an expression for κ as a function of the velocity profile of the system which is scaled by the viscosity of the liquid at 225 K. In doing so, we have obtained an expression for κ which is independent of temperature differences of the liquid water at far displacements from the interface. We found the basal and pyramidal facets to have similar κ values, of $\kappa \approx 0.0006$ (amu Å^{-2} fs^{-1}). However, the prismatic and secondary prismatic facets were found to have κ values of $\kappa \approx 0.0003$ (amu Å^{-2} fs^{-1}). As these ice facets are being sheared relative to liquid water, with the structural and dynamic width of all four interfaces being approximately the same, the difference in the coefficient of friction indicates the hydrophilicity of the crystal facets are not equivalent. Namely, that the basal and pyramidal facets of Ice-I_h are more hydrophilic than the prismatic and secondary prismatic facets.

ACKNOWLEDGMENTS. Support for this project was provided by the National Science Foundation under grant CHE-1362211. Computational time was provided by the Center for Research Computing (CRC) at the University of Notre Dame.

Han and Hale(1992). K. Han and B. N. Hale, "bibfield journal "bibinfo journal Phys. Rev. B" "textbf "bibinfo volume 45," "bibinfo pages 29 ("bibinfo year 1992).

Granasy(1995). L. Granasy, "bibfield journal "bibinfo journal The Journal of Physical Chemistry" "textbf "bibinfo volume 99," "bibinfo pages 14182 ("bibinfo year 1995), http://pubs.acs.org/doi/pdf/10.1021/j100038a061 .

Vanfleet and Mochel(1995). R. R. Vanfleet and J. Mochel, "bibfield journal "bibinfo journal Surface Science" "textbf "bibinfo volume 341," "bibinfo pages 40 ("bibinfo year 1995).

Weber and Stillinger(1983). T. A. Weber and F. H. Stillinger, The Journal of Physical Chemistry, "bibfield journal "bibinfo journal The Journal of Physical Chemistry" "textbf "bibinfo volume 87," "bibinfo pages 4277 ("bibinfo year 1983).

Sakai(1996a). H. Sakai, "bibfield journal "bibinfo journal Surface Science" "textbf "bibinfo volume 348," "bibinfo pages 387 ("bibinfo year 1996"natexlaba).

Sakai(1996b). H. Sakai, "bibfield journal "bibinfo journal Surface Science" "textbf "bibinfo volume 351," "bibinfo pages 285 ("bibinfo year 1996"natexlabb).

Wierzbicki et al.(2007)Wierzbicki, Dalal, Cheatham, Knickelbein, Haymet, and Madura. A. Wierzbicki, P. Dalal, T. E. Cheatham, J. E. Knickelbein, A. D. J. Haymet, and J. D. Madura, "bibfield journal "bibinfo journal Biophysical journal" "textbf "bibinfo volume 93," "bibinfo pages 1442 ("bibinfo year 2007).

Chapsky and Rubinsky(1997). L. Chapsky and B. Rubinsky, "bibfield journal "bibinfo journal FEBS letters" "textbf "bibinfo volume 412," "bibinfo pages 241 ("bibinfo year 1997).

Duman(2001). J. G. Duman, "bibfield journal "bibinfo journal Annual Review of Physiology" "textbf "bibinfo volume 63," "bibinfo pages 327 ("bibinfo year 2001), pMID: 11181959, http://www.annualreviews.org/doi/pdf/10.1146/annurev.physiol.63.1.327 .

Meister et al.(2013)Meister, Ebbinghaus, Xu, Duman, DeVries, Gruebele, Leitner, and Havenith. K. Meister, S. Ebbinghaus, Y. Xu, J. G. Duman, A. DeVries, M. Gruebele, D. M. Leitner, and M. Havenith, "bibfield journal "bibinfo journal Proceedings of the National Academy of Sciences" "textbf "bibinfo volume 110," "bibinfo pages 1617 ("bibinfo year 2013), http://www.pnas.org/content/110/5/1617.full.pdf+html .

Karim, Kay, and Haymet(1990). O. A. Karim, P. A. Kay, and A. D. J. Haymet, "bibfield journal "bibinfo journal The Journal of Chemical Physics" "textbf "bibinfo volume 92," "bibinfo pages 4634 ("bibinfo year 1990).

Gay, Smith, and Haymet(2002). S. C. Gay, E. J. Smith, and A. D. J. Haymet, "bibfield journal "bibinfo journal The Journal of Chemical Physics" "textbf "bibinfo volume 116," "bibinfo pages 8876 ("bibinfo year 2002).

Bryk and Haymet(2002). T. Bryk and A. D. J. Haymet, "bibfield journal "bibinfo journal The Journal of Chemical Physics" "textbf "bibinfo volume 117," "bibinfo pages 10258 ("bibinfo year 2002).

Hayward and Haymet(2001). J. A. Hayward and A. D. J. Haymet, "bibfield journal "bibinfo journal The Journal of Chemical Physics" "textbf "bibinfo volume 114," "bibinfo pages 3713 ("bibinfo year 2001).

Hayward and Haymet(2002). J. A. Hayward and A. D. J. Haymet, "bibfield journal "bibinfo journal Phys. Chem. Chem. Phys." "textbf "bibinfo volume 4," "bibinfo pages 3712 ("bibinfo year 2002).

Karim and Haymet(1988). O. A. Karim and A. D. J. Haymet, "bibfield journal "bibinfo journal The Journal of Chemical Physics" "textbf "bibinfo volume 89," "bibinfo pages 6889 ("bibinfo year 1988).

Bryk and Haymet(2004a). T. Bryk and A. D. J. Haymet, Journal of Molecular Liquids 112, 47 (2004a).

Smith, Bryk, and Haymet(2005). E. J. Smith, T. Bryk, and A. D. J. Haymet, "bibfield journal "bibinfo journal The Journal of Chemical Physics" "textbf "bibinfo volume 123," "bibinfo eid 034706 ("bibinfo year 2005).

Wilson and Haymet(2008). P. W. Wilson and A. D. J. Haymet, "bibfield journal "bibinfo journal The Journal of Physical Chemistry B" "textbf "bibinfo volume 112," "bibinfo pages 11750 ("bibinfo year 2008), pMID: 18720967, http://pubs.acs.org/doi/pdf/10.1021/jp804047x .

Wilson and Haymet(2010). P. W. Wilson and A. D. J. Haymet, "bibfield journal "bibinfo journal The Journal of Physical Chemistry B" "textbf "bibinfo volume 114," "bibinfo pages 12585 ("bibinfo year 2010), http://pubs.acs.org/doi/pdf/10.1021/jp105001c .

Louden and Gezelter(2013). P. B. Louden and J. D. Gezelter, "bibfield journal "bibinfo journal The Journal of Chemical Physics" "textbf "bibinfo volume 139," "bibinfo eid 194710 ("bibinfo year 2013).

Kumar, Buldyrev, and Stanley(2009). P. Kumar, S. V. Buldyrev, and H. E. Stanley, "bibfield journal "bibinfo journal Proceedings of the National Academy of Sciences" "textbf "bibinfo volume 106," "bibinfo pages 22130 ("bibinfo year 2009), http://www.pnas.org/content/106/52/22130.full.pdf+html .

Errington and Debenedetti(2001). J. R. Errington and P. G. Debenedetti, Nature 409, 318 (2001).

Bryk and Haymet(2004b). T. Bryk and A. Haymet, "bibfield journal "bibinfo journal Molecular Simulation" "textbf "bibinfo volume 30," "bibinfo pages 131 ("bibinfo year 2004"natexlabb).

Kuang and Gezelter(2012). S. Kuang and J. D. Gezelter, Molecular Physics 110, 691 (2012).

There is significant interest in the properties of ice/ice and ice/water interfaces in the geophysics community. Most commonly, the results of shearing two ice blocks past one another[**?**, **?**, **?**, **?**] or the shearing of ice through water[**?**, **?**]. Using molecular dynamics simulations, Samadashvili has recently shown that when two smooth ice slabs slide past one another, a stable liquid-like layer develops between them[**?**]. To fundamentally understand these processes, a molecular understanding of the ice/water interfaces is needed.

Investigation of the ice/water interface is also crucial in understanding processes such as nucleation, crystal growth,[11992Han and Hale, 21995Granasy, 31995Vanfleet and Mochel] and crystal melting[41983Weber and Stillinger, 11992Han and Hale, 51996Sakai, 61996Sakai]. Insight gained to these properties can also be applied to biological systems of interest, such as the behavior of the antifreeze protein found in winter flounder,[72007Wierzbicki *et al.*Wierzbicki, Dalal, Cheatham, Knickelbein, Hayn 81997Chapsky and Rubinsky] and certain terrestial arthropods.[92001Duman, 102013Meister *et al.*Meister, Ebbinghaus, Xu, Duman, DeVries, Gruebele, Leitn Elucidating the properties which give rise to these processes through experimental techniques can be expensive, complicated, and sometimes infeasible. However, through the use of molecular dynamics simulations much of the problems of investigating these properties are alleviated.

Understanding ice/water interfaces inherently begins with the isolated systems. There has been extensive work parameterizing models for liquid water, such as the SPC[**?**], SPC/E[**?**], TIP4P[**?**], TIP4P/2005[**?**], (...), and more recently, models for simulating the solid phases of water, such as the TIP4P/Ice[**?**] model. The melting point of various crystal structures of ice have been calculated for many of these models (SPC[111990Karim, Kay, and Haymet, **?**], SPC/E[**?**, **?**, 122002Gay, Smith, and Haymet, 132002Bryk and Haymet, **?**, **?**, **?**, **?**, **?**], TIP4P[161988Karim and Haymet, **?**, **?**, **?**, **?**, **?**, **?**, **?**], TIP5P[**?**, **?**, **?**, **?**, **?**]), and the partial or complete phase diagram for the model has been determined (SPC/E[**?**, **?**, **?**], TIP4P[**?**, **?**, **?**], TIP5P[**?**, **?**]). Knowing the behavior and melting point for these models has enabled an initial investigation of ice/water interfaces.

The Ice-I_h/water quiescent interface has been extensively studied over the past 30 years by theory and experiment. Haymet *et al.* have done significant work characterizing and quantifying the width of these interfaces for the SPC,[111990Karim, Kay, and Haymet] SPC/E,[122002Gay, Smith, and Haymet, 132002Bryk and Haymet], CF1,[142001Hayward and Haymet, 152002Hayward and Haymet] and TIP4P[161988Karim and Haymet] models for water. In recent years, Haymet has focused on investigating the effects cations and anions have on crystal nucleaion and melting.[172004Bryk and Haymet, 182005Smith, Bryk, and Haymet, 192008Wilson and Haymet, 202010Wilson and Haymet] Nada and Furukawa have studied the the basal- and prismatic-water interface width[**?**], crystal surface restructuring at temperatures approaching the melting point[**?**], and the mechanism of ice growth inhibition by antifreeze proteins[**?**, **?**, **?**]. Nada has developed a six-site water model for ice/water interfaces near the melting point[**?**], and studied the dependence of crystal growth shape on applied pressure[**?**]. Using this model, Nada and Furukawa have established differential growth rates for the basal, prismatic, and secondary prismatic facets of Ice-I_h and found their origins due to a reordering of the hydrogen bond network in water near the interface[**?**]. While the work described so far has mainly focused on bulk water on ice, there is significant interest in thin films of water on ice surfaces as well.

It is well known that the surface of ice exhibits a premelting layer at temperatures near the melting point, often called a quasi-liquid layer (QLL). Molecular dynamics simulations of the facets of ice-I_h exposed to vacuum performed by Conde, Vega and Patrykiejew have found QLL widths of approximately 10 Å at 3 K below the melting point[**?**]. Similarly,

Limmer and Chandler have used course grain simulations and statistical field theory to estimated QLL widths at the same temperature to be about 3 nm[**?**]. Recently, Sazaki and Furukawa have developed an experimental technique with sufficient spatial and temporal resolution to visulaize and quantitatively analyze QLLs on ice crystals at temperatures near melting[**?**]. They have found the width of the QLLs perpindicular to the surface at -2.2°C to be $\mathcal{O}$(Å). They have also seen the formation of two immiscible QLLs, which displayed different stabilities and dynamics on the crystal surface[**?**]. Knowledge of the hydrophilicities of each of the crystal facets would help further our understanding of the properties and dynamics of the QLLs.

Presented here is the follow up to our previous paper[212013Louden and Zeeto], in which the basal and prismatic facets of an ice-I_h/water interface were investigated where the ice was sheared relative to the liquid. By using a recently developed velocity shearing and scaling approach to reverse non-equilibrium molecular dynamics (VSS-RNEMD), simultaneous temperature and velocity gradients can be applied to the system, which allows for measurment of friction and thermal transport properties while maintaining a stable interfacial temperature[**?**]. Structural analysis and dynamic correlation functions were used to probe the interfacial response to a shear, and the resulting solid/liquid kinetic friction coefficients were reported. In this paper we present the same analysis for the pyramidal and secondary prismatic facets, and show that the differential interfacial friction coefficients for the four facets of ice-I_h are determined by their relative hydrophilicity by means of dynamics water contact angle simulations.

The local tetrahedral order parameter, $q(z)$, is given by

$$q(z) = \int_0^L \sum_{k=1}^{N} \left(1 - \frac{3}{8} \sum_{i=1}^{3} \sum_{j=i+1}^{4} \left(\cos\psi_{ikj} + \frac{1}{3} \right)^2 \right) \delta(z_k - z) \mathrm{d}z \Big/ N_z \qquad [9]$$

where ψ_{ikj} is the angle formed between the oxygen sites of molecules i,k, and j, where the centeral oxygen is located within molecule k and molecules i and j are two of the closest four water molecules around molecule k. All four closest neighbors of molecule k are also required to reside within the first peak of the pair distribution function for molecule k (typically < 3.41 Å for water). $N_z = \int \delta(z_k - z)\mathrm{d}z$ is a normalization factor to account for the varying population of molecules within each finite-width bin.

The hydrophobicity or hydrophilicity of a surface can be described by the extent a droplet of water wets the surface. The contact angle formed between the solid and the liquid, θ, which relates the free energies of the three interfaces involved, is given by Young's equation.

$$\cos\theta = (\gamma_{sv} - \gamma_{sl})/\gamma_{lv} \qquad [10]$$

Here γ_{sv}, γ_{sl}, and γ_{lv} are the free energies of the solid/vapor, solid/liquid, and liquid/vapor interfaces respectively. Large contact angles ($\theta \gg 90^\circ$) correspond to low wettability and hydrophobic surfaces, while small contact angles ($\theta \ll 90^\circ$) correspond to high wettability and hydrophilic surfaces. Experimentally, measurements of the contact angle of sessile drops has been used to quantify the extent of wetting on surfaces with thermally selective wetting charactaristics[**?**, **?**, **?**], as well as nano-pillared surfaces with electrically tunable Cassie-Baxter and Wenzel states[**?**, **?**, **?**, **?**, **?**]. Luzar and coworkers have done significant work modeling these transitions on nano-patterned surfaces[**?**, **?**, **?**, **?**], and have found the change in contact angle to be due to the external field perturbing the hydrogen bonding of the liquid/vapor interface[**?**].

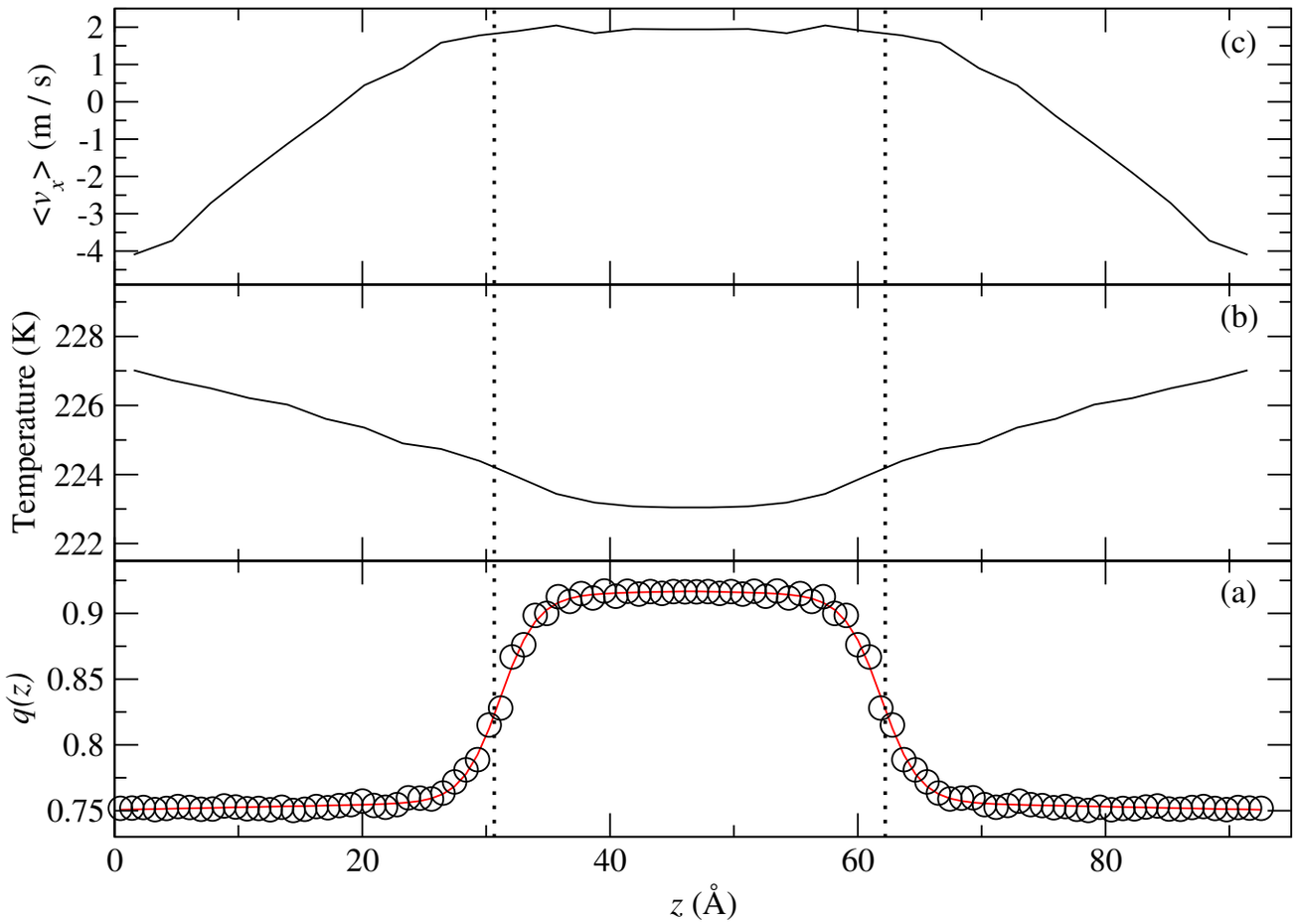

Fig. 1. The pyramidal interface with a shear rate of 3.8 ms^{-1}. Lower panel: the local tetrahedral order parameter, $q(z)$, (black circles) and the hyperbolic tangent fit (red line). Middle panel: the imposed thermal gradient required to maintain a fixed interfacial temperature. Upper panel: the transverse velocity gradient that develops in response to an imposed momentum flux. The vertical dotted lines indicate the locations of the midpoints of the two interfaces.

Table 1. Phyiscal properties of the basal, prismatic, pyramidal, and secondary prismatic facets of Ice-I_h

	$\kappa_{Dragdirection}$ (x10^{-4} amu Å^{-2} fs^{-1})			
Interface	κ_x	κ_y	θ_∞	$K_{spread}(ns^{-1})$
basal	5.9 ± 0.3	6.5 ± 0.8	34.1 ± 0.9	0.60 ± 0.07
pyramidal	5.8 ± 0.4	6.1 ± 0.5	35 ± 3	0.7 ± 0.1
prismatic	3.0 ± 0.2	3.0 ± 0.1	45 ± 3	0.75 ± 0.09
secondary prismatic	3.5 ± 0.1	3.3 ± 0.2	42 ± 2	0.69 ± 0.03

Table 2. Shearing and Droplet simulation parameters

	Shearing			Droplet		
Interface	N_{ice}	N_{liquid}	Lx, Ly, Lz (Å)	N_{ice}	$N_{droplet}$	Lx, Ly (Å)
Basal	900	1846	(23.87, 35.83, 98.64)	12960	2048	(134.70, 140.04)
Prismatic	3000	5464	(35.95, 35.65, 205.77)	9900	2048	(110.04, 115.00)
Pyramidal	1216	2203	(37.47, 29.50, 93.02)	11136	2048	(143.75, 121.41)
Secondary Prismatic	3840	8176	(71.87, 31.66, 161.55)	11520	2048	(146.72, 124.48)

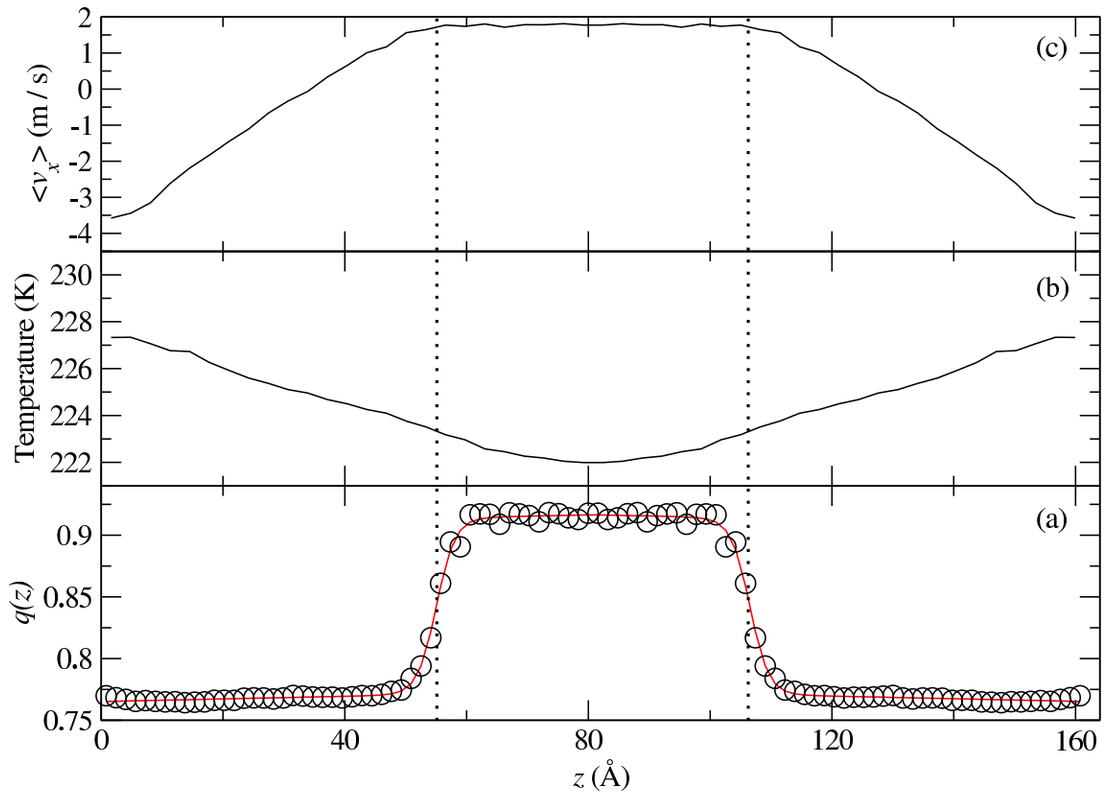

Fig. 2. The secondary prismatic interface with a shear rate of 3.5 ms^{-1}. Panel descriptions match those in figure 1.

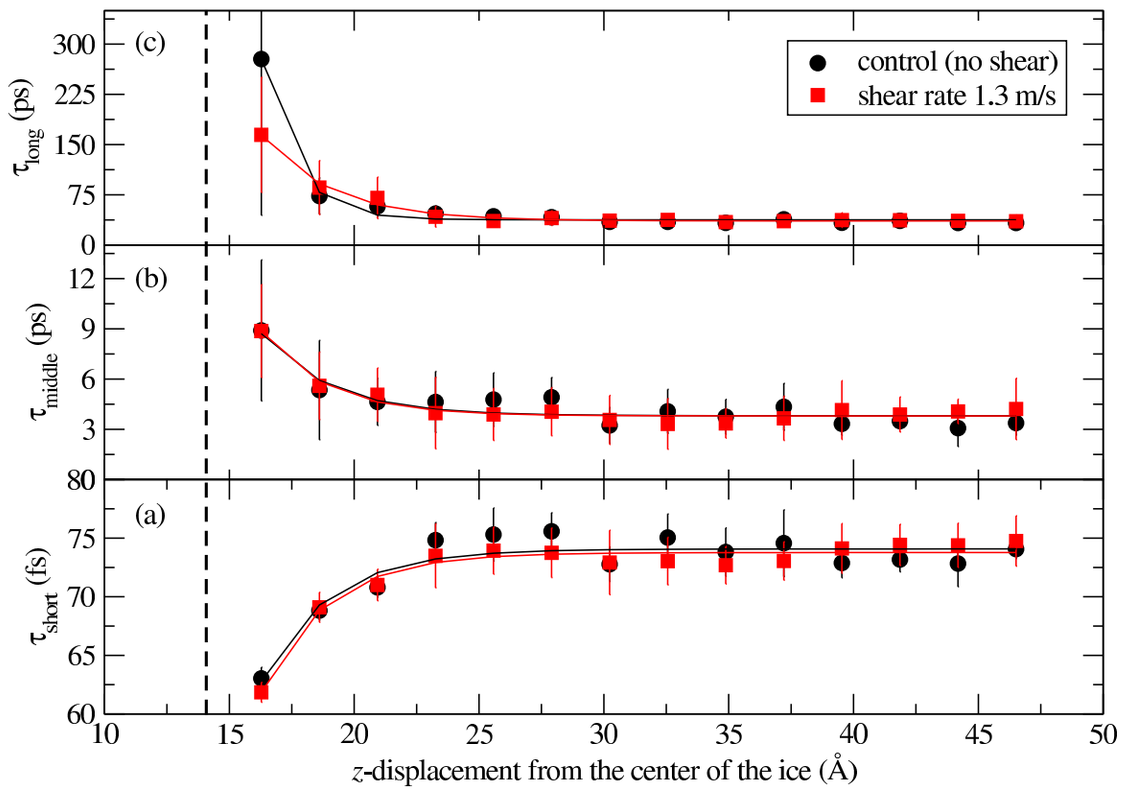

Fig. 3. The three decay constants of the orientational time correlation function, $C_2(t)$, for water as a function of distance from the center of the ice slab. The vertical dashed line indicates the edge of the pyramidal ice slab determined by the local order tetrahedral parameter. The control (black circles) and sheared (red squares) experiments were fit by a shifted exponential decay (Eq. 9[212013Louden and Gezelter]) shown by the black and red lines respectively. The upper two panels show that translational and hydrogen bond making and breaking events slow down through the interface while approaching the ice slab. The bottom most panel shows the librational motion of the water molecules speeding up approaching the ice block due to the confined region of space allowed for the molecules to move in.

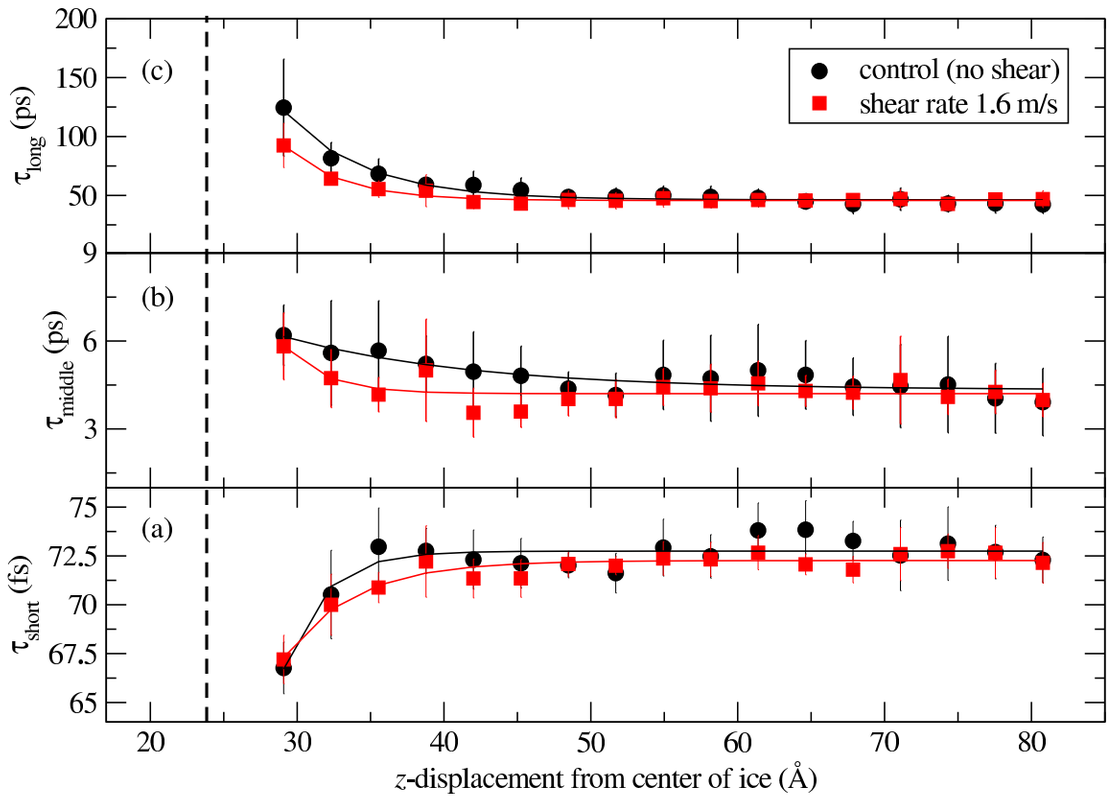

Fig. 4. Decay constants for $C_2(t)$ at the secondary prismatic face. Panel descriptions match those in 3.